

See discussions, stats, and author profiles for this publication at: <https://www.researchgate.net/publication/283582314>

Two-Photon Lithography of 3D Nanocomposite Piezoelectric Scaffolds for Cell Stimulation

ARTICLE *in* ACS APPLIED MATERIALS & INTERFACES · NOVEMBER 2015

Impact Factor: 6.72 · DOI: 10.1021/acsaami.5b08764

READS

73

9 AUTHORS, INCLUDING:



[Barbara Mazzolai](#)

Istituto Italiano di Tecnologia

196 PUBLICATIONS 1,584 CITATIONS

[SEE PROFILE](#)



[Vincenzo Piazza](#)

Istituto Italiano di Tecnologia

72 PUBLICATIONS 555 CITATIONS

[SEE PROFILE](#)



[Massimiliano Labardi](#)

Italian National Research Council

104 PUBLICATIONS 1,065 CITATIONS

[SEE PROFILE](#)



[Virgilio Mattoli](#)

Istituto Italiano di Tecnologia

157 PUBLICATIONS 1,135 CITATIONS

[SEE PROFILE](#)

Two-Photon Lithography of 3D Nanocomposite Piezoelectric Scaffolds for Cell Stimulation

Attilio Marino,^{*,†,‡} Jonathan Barsotti,^{†,‡} Giuseppe de Vito,^{§,⊥} Carlo Filippeschi,[†] Barbara Mazzolai,[†] Vincenzo Piazza,[§] Massimiliano Labardi,^{||} Virgilio Mattoli,[†] and Gianni Ciofani^{*,†,‡}

[†]Center for Micro-BioRobotics @SSSA, Istituto Italiano di Tecnologia, Viale Rinaldo Piaggio 34, 56025 Pontedera, Italy

[‡]The Biorobotics Institute, Scuola Superiore Sant'Anna, Viale Rinaldo Piaggio 34, 56025 Pontedera, Italy

[§]Center for Nanotechnology Innovation @NEST, Istituto Italiano di Tecnologia, Piazza San Silvestro 12, 56127 Pisa, Italy

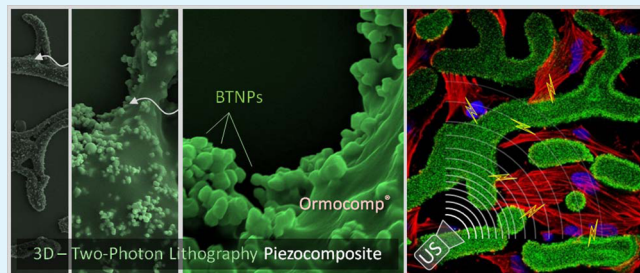
[⊥]NEST, Scuola Normale Superiore, Piazza San Silvestro 12, 56127 Pisa, Italy

^{||}CNR-IPCF, UOS Pisa, Largo Pontecorvo 3, 56127 Pisa, Italy

[#]Department of Mechanical and Aerospace Engineering, Politecnico di Torino, Corso Duca degli Abruzzi 24, 10129 Torino, Italy

Supporting Information

ABSTRACT: In this letter, we report on the fabrication, the characterization, and the in vitro testing of structures suitable for cell culturing, prepared through two-photon polymerization of a nanocomposite resist. More in details, commercially available Ormocomp has been doped with piezoelectric barium titanate nanoparticles, and bioinspired 3D structures resembling trabeculae of sponge bone have been fabricated. After an extensive characterization, preliminary in vitro testing demonstrated that both the topographical and the piezoelectric cues of these scaffolds are able to enhance the differentiation process of human SaOS-2 cells.



KEYWORDS: *two-photon lithography, barium titanate nanoparticles, direct laser writing, piezoelectric stimulation, bone tissue engineering*

Two-photon lithography (TPL) is a disrupting technology that allows the fabrication of complex 3D nanostructured scaffolds, owing to the mechanism of two-photon absorption and polymerization of dedicated photoresists.¹ Obtained 3D structures are suitable for in vitro testing on living cells, and can be exploited for the investigation of cell/substrate biophysical interactions, for the promotion of a specific cell phenotype, and for the modification of surfaces of biomedical devices.^{2,3} As an example, concerning bone tissue engineering we have recently developed 3D structures bioinspired by the geometry of a sponge-bone trabecula, named "Osteo-Prints": these scaffolds have been demonstrated to promote the osteogenic differentiation of SaOS-2 osteoblast-like cells through topographical stimulation.⁴ More in details, the enhanced osteogenesis was proven to be induced by the presence of the 3D biomimetic niches able to affect the cellular (and nuclear) shape and fostering cell commitment toward osteogenesis.

The availability of several materials that can be exploited as photoresists for the TPL allows the control of a wide range of physical/chemical properties of the material (i.e., stiffness, porosity, roughness, biodegradability, etc.), which can be further tuned by doping the resists with appropriate nanomaterials (i.e., single-walled carbon nanotubes,⁵ titanium dioxide nanoparticles,⁶ magnetic nanoparticles,⁷ piezoelectric nanoparticles,⁸ zinc oxide nanowires,⁹ etc.), thus obtaining "smart"

features not achievable by the use of the corresponding bulk material.¹⁰ It is well-known that composite/nanocomposite materials are gaining considerable interest in a wide range of research areas, from the aerospace field to bioapplications, because of the possibility of finely tune their chemical and physical properties.¹¹ Further advancements in the biomedical field are expected, also owing to innovative fabrication approaches, that allow for rapid prototype production.¹² Scaffolds prepared with such nanocomposites can show active/sensitive behaviors, deriving, for example, by the magnetic, conductive, or piezoelectric properties of the exploited nanoparticles; obtained structures can thus be successfully exploited for an active stimulation of cells and, eventually, tissues.

As an example of peculiar 3D nanocomposite structures fabricated by TPL, the Kawata group recently developed a technique to obtain nanocomposites in which the embedded single-walled carbon nanotubes (SWCNTs) are aligned along a desired directions, i.e., along the laser scanning guidance.⁵ Anisotropic structures characterized by aligned SWCNTs are

Received: September 17, 2015

Accepted: November 9, 2015

Published: November 9, 2015



extremely interesting in the field of actuators, besides exhibiting an enhancement of mechanical, electrical, thermal, and optical properties with respect to analogous isotropic constructs. Concerning magnetic structures fabricated by TPL, Wang et al. reported on the remote manipulation through an external ferromagnetic field of microspring-like shaped nanocomposites containing Fe_3O_4 nanoparticles.⁷ Further improvements in this approach allowed for magnetic control of 3D scaffolds fabricated by TPL suitable for stem cell transplantation applications,¹³ and of magnetic helical microswimmers for targeted gene delivery.¹⁴

Focusing on piezoelectric nanomaterials, different cell types (including neurons,¹⁵ neural stem cells,¹⁶ and fibroblasts¹⁷) have been successfully stimulated by taking advantage of nanoparticles/nanofibers showing piezoelectric behavior. Indeed, these nanomaterials are able to generate electricity in response to mechanical deformations, which can be accomplished by using ultrasounds (US).¹⁸ In this context, here we suggest the use of the TPL technique for the fabrication of 3D piezoelectric structures (specifically the above-mentioned Osteo-Prints doped with piezoelectric nanoparticles) in order to further promote and enhance the osteogenic differentiation of SaOS-2 cells.

The preparation of the nanocomposite photoresist was carried out by mixing the commercially available biocompatible Ormocomp resist with piezoelectric barium titanate nanoparticles (BTNPs, 10 wt %). In order to test the obtained nanocomposite photoresist, TPL of a 3D structure resembling the logo of our institute (IIT) was fabricated through the slice-by-slice approach. Figure 1a shows a scanning electron microscopy (SEM) tilted scan of the obtained logo, the surface of which appears particularly rough because of the presence of a large amount of nanoparticles. Single BTNPs on the surface of the IIT logo can be appreciated in Figure 1b. In particular, the left image is a higher-magnification SEM acquisition of a small portion of the previous structure. Energy-dispersive X-ray analysis (EDX) performed on the same scan clearly confirms the presence of nanoparticles on the structure surface, highlighted by the colocalized presence of Ti (in red, image in the middle) and of Ba (in green, image on the right). In order to assess the presence of the nanoparticles in the whole volume of the structure, a focused ion beam was used to mill the structure and analyze its inner composition. The SEM scan (Figure 1c) revealed the presence of the nanoparticles embedded in the polymerized structure, confirmed by the EDX analysis, reported in Figure 1d, that highlighted the presence of the characteristic Ba and Ti peaks at 4.44 and 4.50 keV, respectively (other peaks are related to the silica substrate, to the gold sputtering, and to other elements composing the resist). All together, SEM and EDX characterizations demonstrate the possibility to obtain, by TLP and with high reproducibility, 3D structures composed by Ormocomp and piezoelectric BTNPs (both localized on the surface and embedded inside the structures).

Nanoparticle distribution inside the structures has been investigated also with “nondestructive” methods, taking advantage of the peculiar nonlinear optical properties of the BTNPs.¹⁹ These nanoparticles can be in fact easily imaged by multimodal nonlinear optical microscopy through the detection of the coherent anti-Stokes Raman scattering (CARS) and of the sum frequency generation signal (SFG, Figure 2a–e), and by standard confocal laser scanning microscopy (CLSM, Figure 2f, g).²⁰ Using the multimodal nonlinear optical imaging setup,

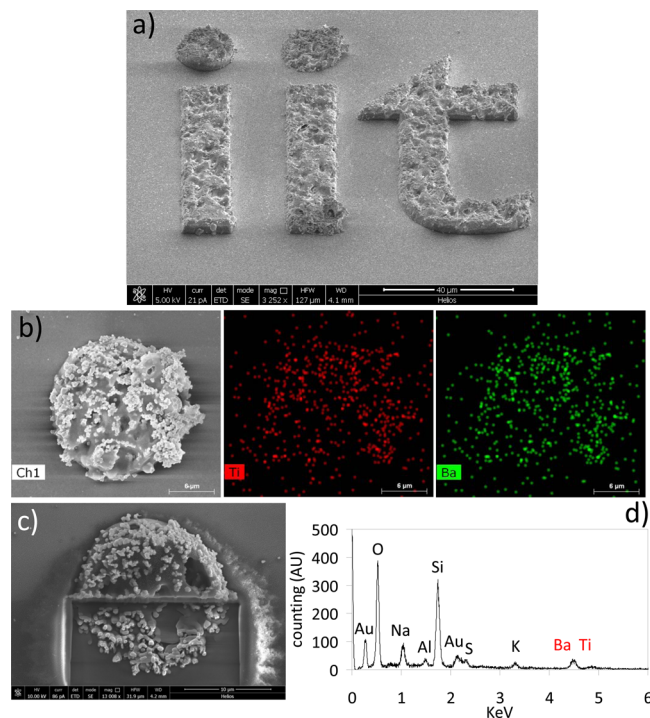


Figure 1. 3D nanocomposite (Ormocomp resist/BTNPs 10 wt %) structures fabricated by two-photon lithography (TPL). (a) The logo of our institute (IIT) was fabricated with a slice-by-slice approach and then imaged with scanning electron microscopy (SEM). (b) The left image is the SEM high-magnification scan of the dot of the letter “I” of the logo; center and left images show the energy-dispersive X-ray analysis (EDX) related, respectively, to the Ti (in red) and Ba (in green) elements, demonstrating the presence of the BTNPs on the surface of the structure. (c) A focused ion beam was used to mill the structure and analyze its inner composition: the SEM scan reveals the presence of the nanoparticles embedded in the polymerized structure; EDX spectrum (d) confirms the presence of the characteristic Ba and Ti peaks at 4.44 and 4.50 keV, respectively.

we visualized both structures polymerized with plain Ormocomp (without BTNPs, Figures 2a), and fabricated with the BTNP-doped resist (Figures 2c, e). Exploiting a Stokes and a pump-and-probe beam (PaPB) exciting lasers at 1060 and 810 nm, respectively, we detected the CARS radiation emitted by the CH_2 bonds of the Ormocomp at 655 nm (in green in the images, emission spectrum reported in Figure 2b) and the SFG radiation emitted by the BTNPs at 460 nm (in red in the images, emission spectrum reported in Figure 2d).^{21,22} The presence of the nanoparticles inside the structure was confirmed by a z-stack acquisition (Figure 2e). Exploiting the CLSM setup, instead, we imaged the BTNPs inside the structure by using an excitation laser at 642 nm and by collecting emitted signal from 670 to 750 nm, as demonstrated by a single slice of a z-stack acquisition (Figure 2f) and by the relative 3D rendering (Figure 2g, pseudocolors have been used to code the depth along the z axis).

The investigation of the material piezoelectricity was performed through piezoresponse force microscopy (PFM). This technique consists in applying an alternating voltage to the cantilever tip while simultaneously measuring the material deformations as a result of the converse piezoelectric effect; further details regarding the adopted PFM system are reported in the Supporting Information. PFM analysis confirms that the nanocomposite material is characterized by a significantly

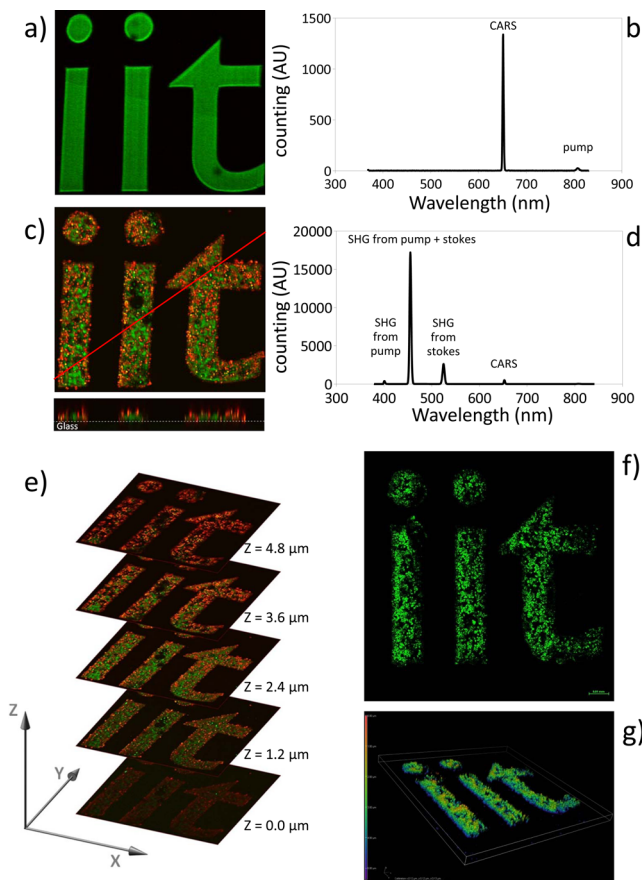


Figure 2. 3D optical characterization of the nanocomposite structures. In (a-e) the multimodal (CARS and SFG) nonlinear optical imaging is reported; the CARS signal (emitted by CH_2 bonds) is mapped in green and the SFG signal (emitted by the BTNPs) in red. (a) XY optical section ($140 \mu\text{m} \times 140 \mu\text{m}$) and (b) emission spectrum of the “control” logo (plain Ormocomp). (c) XY optical section ($140 \mu\text{m} \times 140 \mu\text{m}$) and (d) emission spectrum of the nanocomposite logo (Ormocomp/BTNPs). (e) XY optical sections ($140 \mu\text{m} \times 140 \mu\text{m}$) from a z-stack of the nanocomposite IIT logo. (f, g) Confocal laser scanning microscopy (CLSM) imaging of the nanocomposite logo. (f) Single XY optical section (BTNPs in green) and (g) 3D rendering of the nanocomposite logo (pseudocolors have been used to code the depth along the z axis).

higher d_{33} ($0.57 \pm 0.08 \text{ pm/V}$) compared to that one of the plain Ormocomp without BTNPs ($0.07 \pm 0.01 \text{ pm/V}$): this result suggests that the presence of the BTNPs confers piezoelectric properties to the structure, confirming the success of the proposed approach.

To promote the osteogenic differentiation by combining topographic and piezoelectric stimulations, Osteo-Prints bioinspired by the 3D shape of the bone trabeculae were obtained through the slice-by-slice TPL of the described nanocomposite photoresist (Ormocomp/BTNPs). In Figure 3a, SEM imaging confirms the success of the polymerization process, having obtained structures of well-defined shapes doped with piezoelectric BTNPs, clearly observable at higher magnifications (from left to right increasing magnification SEM images are reported).

Square matrices of repeated Osteo-Prints (located at a $50 \mu\text{m}$ distance from each other) have been developed for extensive biological testing on human osteoblast-like SaOS-2 cells. Figure 3b depicts CLSM acquisitions of SaOS-2 grown for 24 h on the

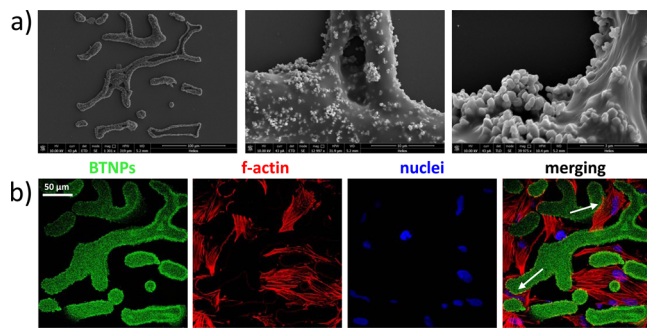


Figure 3. (a) SEM imaging of a nanocomposite Osteo-Print (left); high-magnification images of the Osteo-Print (in the center and in the right) show the presence of the BTNPs on the surface of the 3D structure. (b) Confocal laser scanning microscopy of SaOS-2 osteoblast-like cells cultured on Osteo-Prints; BTNPs in green, f-actin in red, nuclei in blue. White arrows highlight strong interaction cells/scaffolds, affecting cellular shape.

Osteo-Prints: in green we can appreciate the presence of the BTNPs, in red the f-actin of the cell cytoskeleton (stained with TRITC-phalloidin) and in blue the nuclei (DAPI). These images qualitatively reveal as cells make strict connections to the surface of the scaffolds, by conforming their shape to that of the scaffolds (as indicated by white arrow in the images), as already reported in our previous work;⁴ furthermore, they are characterized by elongated/curved-shaped nuclei. As already pointed out, several investigations stressed that nucleus elongation, induced by cell deformation, is associated with chromatin condensation, and thus plays a key role during the process of cellular differentiation, representing a critical step in the mechanotransduction pathway that transduces the topographical cues into altered genic expression.²³

After 24 h from the cell seeding, osteogenesis was induced for 3 days in SaOS-2 cells by using a culture medium supplemented with β -glycerophosphate, dexamethasone, and ascorbic acid (please see the Supporting Information for the details about cell culture/differentiation). During the differentiation, cells were divided into four experimental groups: cells differentiated on (i) control plain Osteo-Prints (OP) (non-doped), (ii) Osteo-Prints doped with piezoelectric nanoparticles (OP/BTNPs), (iii) plain Osteo-Prints stimulated with ultrasounds (OP + US), and (iv) doped Osteo-Prints stimulated with ultrasounds (OP/BTNPs + US). The US stimulation was performed at 0.8 W/cm^2 for 5 s every 4 h, 3 times a day, during the all differentiation periods.

After the stimulation protocol, immunocytochemistry experiments were performed against two markers (Figure 4a, first and second raw), K_i -67 and collagen type 1 (COL1). K_i -67 is a nuclear marker expressed in proliferating cells during G1, S, G2 and M cell cycle phases. Interestingly, the percentage of SaOS-2 cells expressing K_i -67 in response to the OP/BTNPs + US treatment ($40 \pm 3\%$) was significantly lower compared to the other experimental groups (Figure 4b, first plot): OP ($71 \pm 5\%$), OP + US ($62 \pm 5\%$), and OP/BTNPs ($64 \pm 4\%$, Figure 4b). This finding highlights a promotion of the exit from cell cycle when cells underwent the synergic stimulation (OP/BTNPs + US). Moreover, synergic stimulation also affected the expression of COL1 protein, a marker highly up-regulated during osteogenesis.²⁴ Percentage of area occupied by the collagen deposits produced by SaOS-2 differentiated in the OP/BTNPs + US condition was significantly higher ($0.7 \pm 0.2\%$) compared to the other experimental groups (Figure 4b,

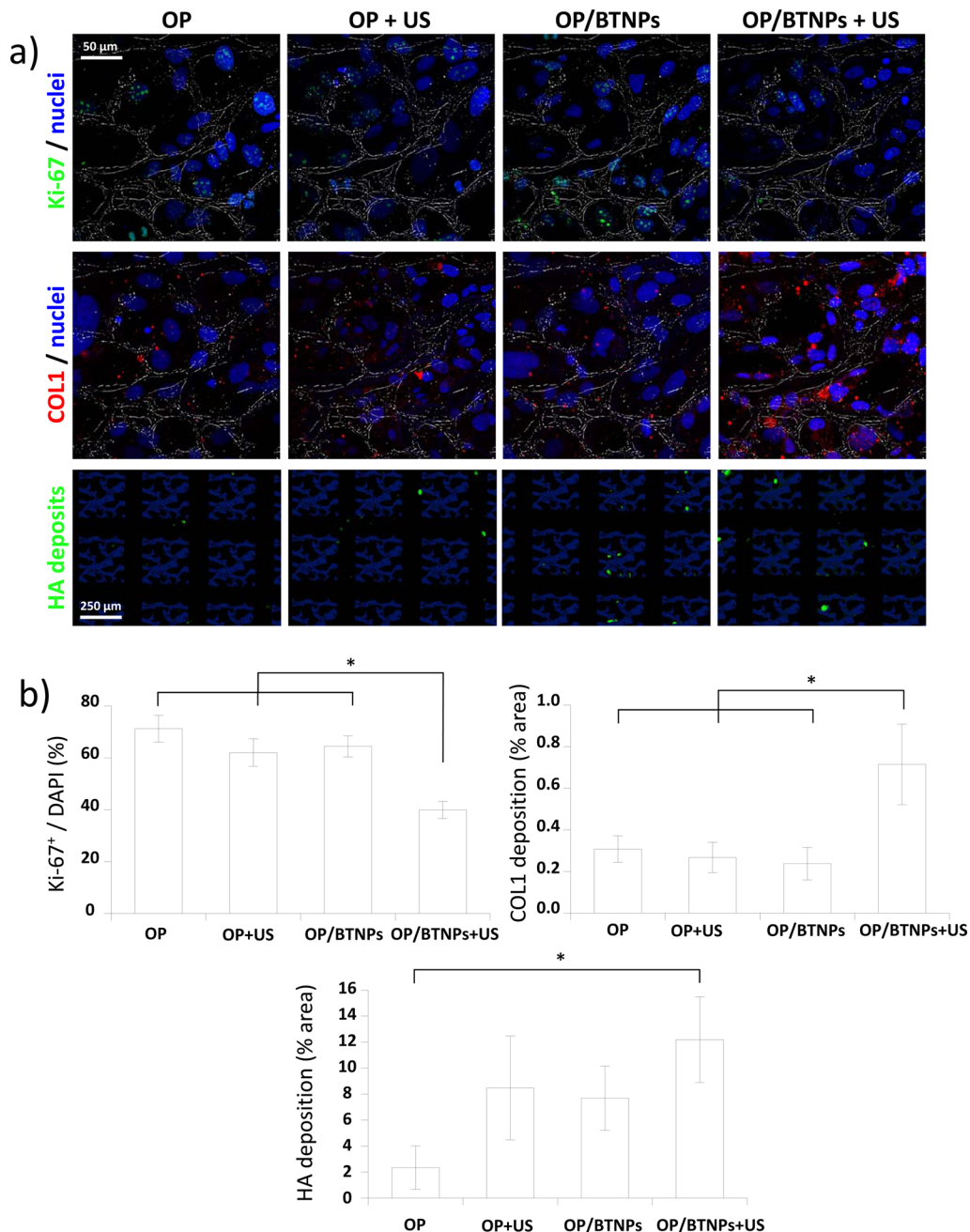


Figure 4. Nanocomposite bioinspired Osteo-Prints for the promotion of the osteogenic differentiation. (a) Confocal laser scanning microscopy images of Ki-67 and collagen type 1 (COL1) and fluorescence microscopy images of hydroxyapatite (HA) in SaOS-2 cultures differentiated on control Osteo-Prints (OP), on nanocomposite Osteo-Prints (OP/BNPs), and that underwent ultrasound stimulation on the two structures (OP + US and OP/BNPs + US). Ki-67 in green, COL1 in red, nuclei in blue, and HA in green. (b) Quantitative analyses of the above-described markers (average \pm standard deviation, * $p < 0.01$).

second plot), namely OP ($0.3 \pm 0.1\%$), OP + US ($0.3 \pm 0.1\%$), and OP/BNPs ($0.2 \pm 0.1\%$).

Finally, osteogenesis progression can be also reliably monitored as a function of the hydroxyapatite (HA) nodules deposition.²⁵ Osteoimage assay was performed to investigate the bone mineralization efficiency (further experimental details available in Supporting Information), in terms of HA deposition in the SaOS-2 cultures (Figure 4a, third row). The percentage area (average \pm standard deviation) occupied by the HA deposits in the 4 experimental groups is reported in the third plot of Figure 4b. The HA deposit area of SaOS-2 in OP + US ($8.5 \pm 4.0\%$) and OP/BNPs ($7.5 \pm 2.5\%$) cultures is

higher, but not significantly different with respect to that one of the OP control experimental group ($2.4 \pm 1.7\%$, $p > 0.05$). Instead, the HA deposition in the OP/BNPs + US group ($12.2 \pm 3.3\%$) was found significantly higher compared to the controls (OP, $p < 0.01$). All together, these results indicate that both the presence of the BNPs in the structures and the US stimulation concur to induce a significant osteogenesis enhancement.

It is possible to assume that a piezoelectric excitation is involved in mediating these effects: indeed, in a recent work, we demonstrated that BNPs, activated with the same US intensities, are able to piezoelectrically stimulate neural

cells.²⁰ In this context, it is well-known from the literature that electric stimulation is able to promote osteogenesis, both in vitro²⁶ and in vivo,²⁷ thus a realistic scenario envisages an US-activation of the BTNPs on the OP, that are able to give electric stimuli to the cells, thus enhancing the differentiation process. However, besides piezoelectricity, other phenomena may contribute to the observed osteogenesis enhancement, as a temperature increase and the mechanostimulation of the US, or the roughness due to the presence of the BTNPs on the OP surface. Concerning mechanical stimulation, several examples in the literature suggest the important role played by this physical cue as an anabolic agent for bone regeneration.²⁸ Among mechanical stimuli, US in particular result able of inhibiting the adipogenic differentiation and promoting osteogenesis of mesenchymal stem cells by acting on the ROCK-Cot/Tpl2-MEK-ERK pathway.²⁹ Further efforts will be thus devoted in future works in order to deeply investigate the role of the different mechanisms mediating the osteogenic enhancement in response to the synergic OP/BTNPs + US stimulation.

Concluding, we exploited for the first time the TPL technique to fabricate bioinspired 3D structures (Osteo-Prints) with a nanocomposite resist (Ormocomp/BTNPs). Complementary methods (SEM, FIB, EDX, CARS, SFG, CLSM, and PFM) allowed a deep characterization of the obtained structures. These scaffolds, in concomitance with a mechanical stimulation provided by US, resulted able to enhance the osteogenic differentiation of SaOS-2 bone-like cells. Obtained findings open new interesting perspectives in the field of regenerative medicine and bone tissue engineering: as an example, the possibility to functionalize the surface of biomedical devices with biomimetic piezoelectric structures can potentially foster the osseointegration of the implants, by combining the US-driven piezoelectric stimulation with the presence of a bioinspired topography. This is a unique opportunity that is not offered, for example, by traditional titanium- and carbon-based materials: BTNP-based nanocomposites, with respect to other nanostructured materials adopted for bone tissue engineering,³⁰ not only mimic the piezoelectric properties of the bone, but they can be also remotely actuated for promoting the osseointegration/bone regeneration.

ASSOCIATED CONTENT

Supporting Information

The Supporting Information is available free of charge on the ACS Publications website at DOI: [10.1021/acsami.5b08764](https://doi.org/10.1021/acsami.5b08764).

More details of the experimental methods used; paragraphs concerning structure fabrication and characterization, biological experiments, and relevant analysis ([PDF](#))

AUTHOR INFORMATION

Corresponding Authors

*E-mail: attilio.marino@iit.it.

*E-mail: gianni.ciofani@polito.it.

Notes

The authors declare no competing financial interest.

ACKNOWLEDGMENTS

This research has been partially supported by the Italian Ministry of Health, Grant RF-2011-02350464.

REFERENCES

- (1) Cumpston, B. H.; Ananthavel, S. P.; Barlow, S.; Dyer, D. L.; Ehrlich, J. E.; Erskine, L. L.; Heikal, A. A.; Kuebler, S. M.; Lee, I.-Y. S.; McCord-Maughon, D.; Qin, J.; Röckel, H.; Rumi, M.; Wu, X.-L.; Marder, S. R.; Perry, J. W. Two-Photon Polymerization Initiators for Three-Dimensional Optical Data Storage and Microfabrication. *Nature* **1999**, *398*, 51–54.
- (2) Hribar, K. C.; Soman, P.; Warner, J.; Chung, P.; Chen, S. Light-Assisted Direct-Write of 3D Functional Biomaterials. *Lab Chip* **2014**, *14*, 268–275.
- (3) Raimondi, M. T.; Eaton, S. M.; Nava, M. M.; Laganà, M.; Cerullo, G.; Osellame, R. Two-Photon Laser Polymerization: From Fundamentals to Biomedical Application in Tissue Engineering and Regenerative Medicine. *J. Appl. Biomater. Funct. Mater.* **2012**, *10*, 56–66.
- (4) Marino, A.; Filippeschi, C.; Genchi, G. G.; Mattoli, V.; Mazzolai, B.; Ciofani, G. The Osteoprint: A Bioinspired Two-Photon Polymerized 3-D Structure for the Enhancement of Bone-like Cell Differentiation. *Acta Biomater.* **2014**, *10*, 4304–4313.
- (5) Ushiba, S.; Shoji, S.; Masui, K.; Kono, J.; Kawata, S. Direct Laser Writing of 3D Architectures of Aligned Carbon Nanotubes. *Adv. Mater.* **2014**, *26*, 5653–5657.
- (6) Duan, X.-M.; Sun, H.-B.; Kaneko, K.; Kawata, S. Two-Photon Polymerization of Metal Ions Doped Acrylate Monomers and Oligomers for Three-Dimensional Structure Fabrication. *Thin Solid Films* **2004**, *453–454*, 518–521.
- (7) Wang, J.; Xia, H.; Xu, B.-B.; Niu, L.-G.; Wu, D.; Chen, Q.-D.; Sun, H.-B. Remote Manipulation of Micronanomachines Containing Magnetic Nanoparticles. *Opt. Lett.* **2009**, *34*, 581–583.
- (8) Kim, K.; Zhu, W.; Qu, X.; Aaronson, C.; McCall, W. R.; Chen, S.; Sribny, D. J. 3D Optical Printing of Piezoelectric Nanoparticle-Polymer Composite Materials. *ACS Nano* **2014**, *8*, 9799–9806.
- (9) Fonseca, R. D.; Correa, D. S.; Paris, E. C.; Tribuzi, V.; Dev, A.; Voss, T.; Aoki, P. H. B.; Constantino, C. J. L.; Mendonça, C. R. Fabrication of Zinc Oxide Nanowires/polymer Composites by Two-Photon Polymerization. *J. Polym. Sci., Part B: Polym. Phys.* **2014**, *52*, 333–337.
- (10) Farsari, M.; Vamvakaki, M.; Chichkov, B. N. Multiphoton Polymerization of Hybrid Materials. *J. Opt.* **2010**, *12*, 124001.
- (11) Gloria, A.; Ronca, D.; Russo, T.; D'Amora, U.; Chierchia, M.; De Santis, R.; Nicolais, L.; Ambrosio, L. Technical Features and Criteria in Designing Fiber-Reinforced Composite Materials: From the Aerospace and Aeronautical Field to Biomedical Applications. *J. Appl. Biomater. Biomech.* **2011**, *9*, 151–163.
- (12) De Santis, R.; Russo, A.; Gloria, A.; D'Amora, U.; Russo, T.; Panseri, S.; Sandri, M.; Tampieri, A.; Marcacci, M.; Dedi, V. A.; Wilde, C. J.; Ambrosio, L. Towards the Design of 3D Fiber-Deposited Poly(ϵ -Caprolactone)/Iron-Doped Hydroxyapatite Nanocomposite Magnetic Scaffolds for Bone Regeneration. *J. Biomed. Nanotechnol.* **2015**, *11*, 1236–1246.
- (13) Kim, S.; Qiu, F.; Kim, S.; Ghanbari, A.; Moon, C.; Zhang, L.; Nelson, B. J.; Choi, H. Fabrication and Characterization of Magnetic Microrobots for Three-Dimensional Cell Culture and Targeted Transportation. *Adv. Mater.* **2013**, *25*, 5863–5868.
- (14) Qiu, F.; Fujita, S.; Mhanna, R.; Zhang, L.; Simona, B. R.; Nelson, B. J. Magnetic Helical Microswimmers Functionalized with Lipoplexes for Targeted Gene Delivery. *Adv. Funct. Mater.* **2015**, *25*, 1666–1671.
- (15) Royo-Gascon, N.; Wininger, M.; Scheinbeim, J. I.; Firestein, B. L.; Craielius, W. Piezoelectric Substrates Promote Neurite Growth in Rat Spinal Cord Neurons. *Ann. Biomed. Eng.* **2013**, *41*, 112–122.
- (16) Lee, Y.-S.; Arinze, T. L. The Influence of Piezoelectric Scaffolds on Neural Differentiation of Human Neural Stem/progenitor Cells. *Tissue Eng., Part A* **2012**, *18*, 2063–2072.
- (17) Guo, H.-F.; Li, Z.-S.; Dong, S.-W.; Chen, W.-J.; Deng, L.; Wang, Y.-F.; Ying, D.-J. Piezoelectric PU/PVDF Electrospun Scaffolds for Wound Healing Applications. *Colloids Surf, B* **2012**, *96*, 29–36.

- (18) Wang, X.; Song, J.; Liu, J.; Wang, Z. L. Direct-Current Nanogenerator Driven by Ultrasonic Waves. *Science* **2007**, *316*, 102–105.
- (19) Staedler, D.; Magouroux, T.; Hadji, R.; Joulaud, C.; Extermann, J.; Schwung, S.; Passemard, S.; Kasparyan, C.; Clarke, G.; Gerrmann, M.; Le Dantec, R.; Mugnier, Y.; Rytz, D.; Ciepielewski, D.; Galez, C.; Gerber-Lemaire, S.; Juillerat-Jeanneret, L.; Bonacina, L.; Wolf, J.-P. Harmonic Nanocrystals for Biolabeling: A Survey of Optical Properties and Biocompatibility. *ACS Nano* **2012**, *6*, 2542–2549.
- (20) Marino, A.; Arai, S.; Hou, Y.; Sinibaldi, E.; Pellegrino, M.; Chang, Y.-T.; Mazzolai, B.; Mattoli, V.; Suzuki, M.; Ciofani, G. Piezoelectric Nanoparticle-Assisted Wireless Neuronal Stimulation. *ACS Nano* **2015**, *9*, 7678–7689.
- (21) Rocca, A.; Marino, A.; Rocca, V.; Moscato, S.; de Vito, G.; Piazza, V.; Mazzolai, B.; Mattoli, V.; Ngo-Anh, T. J.; Ciofani, G. Barium Titanate Nanoparticles and Hypergravity Stimulation Improve Differentiation of Mesenchymal Stem Cells into Osteoblasts. *Int. J. Nanomed.* **2015**, *10*, 433–445.
- (22) Farrokhtakin, E.; Ciofani, G.; Puleo, G. L.; de Vito, G.; Filippeschi, C.; Mazzolai, B.; Piazza, V.; Mattoli, V. Barium Titanate Core–Gold Shell Nanoparticles for Hyperthermia Treatments. *Int. J. Nanomed.* **2013**, *8*, 2319–2331.
- (23) Martins, R. P.; Finan, J. D.; Guilak, F.; Lee, D. A. Mechanical Regulation of Nuclear Structure and Function. *Annu. Rev. Biomed. Eng.* **2012**, *14*, 431–455.
- (24) Liskova, J.; Babchenko, O.; Varga, M.; Kromka, A.; Hadraba, D.; Svindrych, Z.; Burdikova, Z.; Bacakova, L. Osteogenic Cell Differentiation on H-Terminated and O-Terminated Nanocrystalline Diamond Films. *Int. J. Nanomed.* **2015**, *10*, 869–884.
- (25) Müller, W. E. G.; Schröder, H. C.; Schlossmacher, U.; Grebenjuk, V. A.; Ushijima, H.; Wang, X. Induction of Carbonic Anhydrase in SaOS-2 Cells, Exposed to Bicarbonate and Consequences for Calcium Phosphate Crystal Formation. *Biomaterials* **2013**, *34*, 8671–8680.
- (26) Kim, I. S.; Song, J. K.; Song, Y. M.; Cho, T. H.; Lee, T. H.; Lim, S. S.; Kim, S. J.; Hwang, S. J. Novel Effect of Biphasic Electric Current on in Vitro Osteogenesis and Cytokine Production in Human Mesenchymal Stromal Cells. *Tissue Eng., Part A* **2009**, *15*, 2411–2422.
- (27) Fredericks, D. C.; Smucker, J.; Petersen, E. B.; Bobst, J. A.; Gan, J. C.; Simon, B. J.; Glazer, P. Effects of Direct Current Electrical Stimulation on Gene Expression of Osteopromotive Factors in a Posterolateral Spinal Fusion Model. *Spine* **2007**, *32*, 174–181.
- (28) Ozcivici, E.; Luu, Y. K.; Adler, B.; Qin, Y.-X.; Rubin, J.; Judex, S.; Rubin, C. T. Mechanical Signals as Anabolic Agents in Bone. *Nat. Rev. Rheumatol.* **2010**, *6*, 50–59.
- (29) Kusuyama, J.; Bandow, K.; Shamoto, M.; Kakimoto, K.; Ohnishi, T.; Matsuguchi, T. Low Intensity Pulsed Ultrasound (LIPUS) Influences the Multilineage Differentiation of Mesenchymal Stem and Progenitor Cell Lines through ROCK-Cot/Tpl2-MEK-ERK Signaling Pathway. *J. Biol. Chem.* **2014**, *289*, 10330–10344.
- (30) Sahoo, N. G.; Pan, Y. Z.; Li, L.; He, C. B. Nanocomposites for Bone Tissue Regeneration. *Nanomedicine* **2013**, *8*, 639–653.